THE JOURNAL OF BIOLOGICAL CHEMISTRY VOL. 285, NO. 46, pp. 35479–35487, November 12, 2010

eNOS-β-Actin Interaction Contributes to Increased Peroxynitrite Formation during Hyperoxia in Pulmonary Artery Endothelial Cells and Mouse Lungs*[S]

Received for publication, May 4, 2010, and in revised form, August 9, 2010 Published, JBC Papers in Press, September 7, 2010, DOI 10.1074/jbc.M110.140269

Dmitry Kondrikov[‡], Shawn Elms[§], David Fulton[‡§], and Yunchao Su[‡§¶‖1]

From the Departments of [‡]Pharmacology and Toxicology and [¶]Medicine, [§]Vascular Biology Center, and [‖]Center for Biotechnology & Genomic Medicine, Medical College of Georgia, Augusta, Georgia 30912

Oxygen toxicity is the most severe side effect of oxygen therapy in neonates and adults. Pulmonary damage of oxygen toxicity is related to the overproduction of reactive oxygen species (ROS). In the present study, we investigated the effect of hyperoxia on the production of peroxynitrite in pulmonary artery endothelial cells (PAEC) and mouse lungs. Incubation of PAEC under hyperoxia (95% O_2) for 24 h resulted in an increase in peroxynitrite formation. Uric acid, a peroxynitrite scavenger, prevented hyperoxia-induced increase in peroxynitrite. The increase in peroxynitrite formation is accompanied by increases in nitric oxide (NO) release and endothelial NO synthase (eNOS) activity. We have previously reported that association of eNOS with β-actin increases eNOS activity and NO production in lung endothelial cells. To study whether eNOS-β-actin association contributes to increased peroxynitrite production, eNOS-β-actin interaction were inhibited by reducing β-actin availability or by using a synthetic peptide (P326TAT) containing a sequence corresponding to the actin binding site on eNOS. We found that disruption of eNOS-β-actin interaction prevented hyperoxia-induced increases in eNOS-β-actin association, eNOS activity, NO and peroxynitrite production, and protein tyrosine nitration. Hyperoxia failed to induce the increases in eNOS activity, NO and peroxynitrite formation in COS-7 cells transfected with plasmids containing eNOS mutant cDNA in which amino acids leucine and tryptophan were replaced with alanine in the actin binding site on eNOS. Exposure of mice to hyperoxia resulted in significant increases in eNOS-β-actin association, eNOS activity, and protein tyrosine nitration in the lungs. Our data indicate that increased association of eNOS with β-actin in PAEC contributes to hyperoxia-induced increase in the production of peroxynitrite which may cause nitrosative stress in pulmonary vasculature.

Oxygen therapy is an important element of the management of various conditions such as adult or neonatal respiratory distress syndrome, circulatory shock, infection, multiple-organ failure syndrome, and pulmonary hypertension (1–6). However, prolonged exposure to increased concentrations of oxygen induces diffuse pulmonary injuries, excessive inflammation, and lung fibrosis. The hyperoxia-induced damages to lung cells have been attributed to the generation of reactive oxygen species (ROS)[2] and subsequent formation of more potent oxidants such as peroxynitrite ($ONOO^-$) (7, 8).

Several studies have suggested that endothelial nitric-oxide synthase (eNOS) plays an important role in the pathogenesis of oxygen toxicity (8, 9). It has been reported that hyperoxia increases eNOS activity and nitric oxide (NO) release from endothelial cells (9, 10). Inhibition of eNOS using L-NAME or knock-out of eNOS reduces peroxynitrite-mediated cytotoxicity in hyperoxic cellular damage in retina (9, 11). However, the mechanism for hyperoxia-induced increases in eNOS activity and NO release has not been clarified. In the present study, we found that exposure of pulmonary artery endothelial cells (PAEC) to hyperoxia (95% O_2 and 5% CO_2) induces increases in eNOS activity and NO release without changes in eNOS protein content, suggesting that hyperoxia increases eNOS activity through a post-translational mechanism.

Protein-protein interactions represent an important post-translational mechanism for eNOS regulation (12). It has been known that calmodulin serves as an allosteric activator for eNOS and that caveolin directly interacts with and inhibits eNOS (13). Bradykinin B2 receptors reside in endothelial caveolae and interact with eNOS in a ligand- and calcium-dependent manner (14). The binding of Ca^{+2}-calmodulin to eNOS disrupts the inhibitory eNOS-caveolin and eNOS-bradykinin B2 complexes, leading to enzyme activation. Hsp90 also serves as an allosteric activator of eNOS (15, 16). Dynamin-2 binds to the FAD binding region of the eNOS reductase domain and potentiates eNOS activity by promoting electron transfer (17). We have reported that eNOS is associated with β-actin in lung endothelial cells and that association of eNOS with β-actin increases eNOS activity and NO release (18–20). The actin binding site on eNOS protein has been identified as being at amino acid residues 326–333 and hydrophobic residues leucine 326, leucine 328, tryptophan 330, and leucine 333 in the actin binding site are essential for actin binding (21). In the

* This work was supported, in whole or in part, by National Institutes of Health Grant R01HL088261. This work was also supported by Flight Attendants Medical Research Institute Grant 072104, and American Heart Association Greater Southeast Affiliate Grants 0555322B and 0855338E.

[S] The on-line version of this article (available at http://www.jbc.org) contains supplemental Figs. S1 and S2.

[1] To whom correspondence should be addressed: Dept. of Pharmacology & Toxicology, Medical College of Georgia, 1120 15th St., Augusta, GA 30912. Tel.: 706-721-7641; Fax: 706-721-2347; E-mail: ysu@mcg.edu.

[2] The abbreviations used are: ROS, reactive oxygen species; NO, nitric oxide; NOS, nitric-oxide synthase; eNOS, endothelial NOS; nNOS, neuronal NOS; iNOS, inducible NOS; $ONOO^-$, peroxynitrite; APF, aminophenyl fluorescein; DHE, dihydroethidine; Hsp90, heat shock protein 90; L-NAME, N^G-nitro-L-arginine methyl ester.

present study, we further evaluated the role of eNOS-β-actin interaction in hyperoxia-induced increases in eNOS activity, NO release, and peroxynitrite formation. We found that hyperoxia increases eNOS-β-actin association and that inhibition of eNOS-β-actin interaction prevents hyperoxia-induced increases in eNOS activity, NO release, peroxynitrite formation, and protein tyrosine nitration in PAEC, suggesting that eNOS-β-actin interaction contributes to increased peroxynitrite formation in PAEC during hyperoxia. Exposure of mice to hyperoxia (85% O_2) resulted in significant increases in eNOS-β-actin association, eNOS activity, and protein tyrosine nitration in the lungs. These observations provided not only new information for the mechanism of hyperoxic nitrosative stress but also the rational to manipulate eNOS-β-actin association to prevent the cellular injuries at hyperoxic condition.

EXPERIMENTAL PROCEDURES

Reagents and Materials—Mouse anti-eNOS and anti-Hsp90 antibodies were obtained from Transduction Laboratory (Lexington, KY). Anti-β-actin monoclonal antibody was obtained from Sigma. Antibodies against eNOS phosphorylated at serine 1177 and threonine 495 were from Cell Signaling Technology (Denvers, MA). nNOS antibody was from Millipore. iNOS antibody was from BD Transduction. β-Actin siRNA was from Ambion (Austin, TX). Anti-nitrotyrosine antibody is from Cayman Chemical (Ann Arbor, MI). Aminophenyl fluorescein (APF) was from Enzo Life Sciences International (Farmingdale, NY). Other reagents were purchased from Sigma.

Cell Culture and Hyperoxic Exposure—Endothelial cells (PAEC) were obtained from the main pulmonary artery of 6–7-month-old pigs and were cultured as previously reported (22). Third- to sixth-passage cells in monolayer culture were maintained in RPMI 1640 medium containing 4% fetal bovine serum and antibiotics (10 units/ml penicillin, 100 μg/ml streptomycin, 20 μg/ml gentamicin, and 2 μg/ml Fungizone) and were used 2 or 3 days after confluence. For hyperoxic exposure, the confluent monolayers of PAEC were incubated at 37 °C to 95% O_2-5% CO_2 (hyperoxia) or air-5% CO_2 (normoxia) at 1 atmosphere for 1–24 h.

Measurement of Peroxynitrite and Protein Tyrosine Nitration—Peroxynitrite was measured as described by Saito *et al.* (23). Briefly, after hyperoxic exposure, endothelial cells were washed with warmed modified Hank's balanced salt solution and were loaded with APF (aminophenyl fluorescein, 10 μM) by incubation for 30 min at 37 °C. After the second wash, fluorescence images were acquired using a confocal laser scanning microscope LSM 510 (Carl Zeiss Co, Ltd.). The excitation and emission wavelengths were 490 and 515 nm. Alternatively, fluorescence intensity of hyperoxia-exposed cells plated in 24-well plates loaded with APF (10 μM) in the presence and absence of uric acid was assayed using SpectraMax spectrophotometer (Molecular Devices, Sunnyvale, CA). Protein tyrosine nitration was measured by Western blot using anti-nitrotyrosine antibody.

Measurement of Superoxide Radicals—After hyperoxic exposure, cells were loaded with 10 μM dihydroethidine (DHE) for 30 min. After washing, fluorescence images were acquired using a confocal laser scanning microscope LSM 510. The excitation and emission wavelengths were 510 nm and 590 nm. Alternatively, fluorescence intensity of hyperoxia-exposed cells plated in 24-well plates loaded with DHE (10 μM) in the presence and absence of tiron was assayed using SpectraMax spectrophotometer.

Determination of eNOS Catalytic Activity and NO Production—After exposure to normoxic or hyperoxic environments, the PAEC monolayers were scraped and homogenized in buffer A (50 mM Tris·HCl, pH 7.4, containing 0.1 mM each EDTA and EGTA, 1 mM phenylmethylsulfonyl fluoride, 1.0 μg/ml leupeptin, and 10 μM calpain inhibitor I). The homogenates were centrifuged at 100,000 g for 60 min at 4 °C, and the total membrane pellet was resuspended in buffer B (buffer A plus 2.5 mM $CaCl_2$). The resulting suspension was used for determination of eNOS activity by monitoring the formation of L-[^{3}H]citrulline from L-[^{3}H]arginine (19). To determine NO production, thapsigargin (100 nM) was added to the medium of endothelial cells following normoxic or hyperoxic exposure. After 60 min of incubation, culture medium was collected and ethanol-precipitated to remove proteins. 50 μl of the reaction mix were loaded to the SIEVERS machine for NO_x (NO_2 and NO_3) measurement according to standard manufacturer's instruction as previously described (24). Protein contents in the cell lysates were determined by Lowry's method.

Co-immunoprecipitation of eNOS and β-Actin—The PAEC lysates were incubated with anti-eNOS antibody, non-immune IgG at 4 °C overnight. 30 μl of protein A-Sepharose was added, and samples were further incubated for 2 h at 4 °C. Immunoprecipitates were collected by centrifugation and washed three times in buffer containing 50 mM Tris-HCl, pH 7.5, 150 mM NaCl, and 0.1% Triton X-100. Proteins were eluted from Sepharose beads by boiling the samples in 30 μl of SDS immunoblotting sample buffer. Sepharose beads were pelleted by centrifugation at 10,000 × *g*, and supernatants were analyzed for eNOS and β-actin by Western blotting.

Immunofluorescence Confocal Microscopy—Confluent control PAEC or PAEC exposed to hyperoxia (95% O_2 and 5% CO_2, 24 h) were fixed in 4% paraformaldehyde and then incubated with 0.1% Triton X-100 for 10 min and with 5% goat serum for 30 min. eNOS and F-actin were then stained with mouse anti-eNOS antibody labeled with FITC-goat anti-mouse IgG and Texas red-phalloidin. After the unbound molecules were washed off, eNOS and actin immunofluorescence were assessed using a Zeiss LSM 510 laser scanning confocal microscope.

Transfection of β-Actin siRNA—To reduce β-actin availability to eNOS, the β-actin mRNA was silenced using its siRNA as previously reported by us (18). Pre-confuorescent PAEC were transfected with 1 μg of β-actin siRNA or a scramble control siRNA (Silencer β-actin siRNA kit, Ambion) using Qiagen RNAiFest transfection reagent in RPMI containing 4% FBS according to the manufacturer's protocol. The ratio of siRNA to transfection reagent was 1:3. Three days after transfection, PAEC were exposed to hyperoxia or normoxia before being used for co-immunoprecipitation and assays of eNOS activity and NO and peroxynitrite formation. Cell number, protein content, and LDH release are comparable between cells transfected with β-actin siRNA and scramble control siRNA sug-

gesting that the injury of β-actin knock-down to PAEC is minimal (18).

Inhibition of eNOS-β-Actin Interaction using Peptide—The actin binding site on eNOS protein has been identified as being at amino acid residues 326–333 and hydrophobic residues leucine 326, leucine 328, tryptophan 330, and leucine 333 in the actin binding site are essential for actin binding (21). To study the role of eNOS-β-actin interaction on eNOS activity, NO release, and peroxynitrite formation, peptide (P326TAT) with amino acid sequence corresponding to the actin binding region of eNOS residues 326–333 linked to an 10 amino acid transduction domain of HIV TAT (RKKRRQRRRA) was synthesized by GeneScript Corporation (Piscataway, NJ). A modified version of ABS peptide 326 with hydrophobic leucine and tryptophan substituted for neutrally charged alanine was used as a control peptide. The amino acid sequences of the peptides are RKKRRQRRRALGLRWYAL for P326TAT and RKKRRQRRRAAGARAYAA for control peptide (PlwTAT). PAEC were incubated with P326TAT or PlwTAT at 20 μM final concentration in MEM medium. After 1 h initial transfection, RPMI medium containing 4% FBS was added to reach final concentration of 2% FBS. Cells were then exposed to hyperoxia or normoxia before being used for co-immunoprecipitation and assays of eNOS activity, NO and peroxynitrite formation, and protein tyrosine nitration.

Site-directed Mutagenesis of eNOS and Transfection of COS-7 Cells with Wild Type and eNOS Mutant—We have reported that hydrophobic residues leucine 326, leucine 328, tryptophan 330, and leucine 333 in the actin binding site are critical for eNOS-β-actin interaction. To study the role of eNOS-β-actin interaction on eNOS activity, NO release, and peroxynitrite formation, residues leucine 326, leucine 328, tryptophan 330, and leucine 333 in the actin binding site were replaced with alanine by using site-directed mutagenesis as described previously (21). Plasmids containing wild type eNOS cDNA or eNOS mutant cDNA were transfected into COS-7 cells using Lipofectamine LTX with PLUS reagent (Invitrogen, Carlsbad, CA) according to the manufacturer's protocol. 48 h after transfection, cells were exposed to hyperoxia or normoxia and then subjected to eNOS-β-actin co-immunoprecipitation and assays for eNOS activity, NO generation, and peroxynitrite formation.

Exposure of Mice to Hyperoxia—Male C57BL/6 mice were purchased from the Jackson Laboratory (Bar Harbor, ME). Animals with ages between 8 and 10 weeks were used. All experiments were performed in accordance with the guiding principles of the Guide for the Care and Use of Laboratory Animals and approved by the Institutional Animal Care and Use Committee (IACUC) of the Medical College of Georgia. Mice were exposed to hyperoxia in a clear plastic polypropylene chamber (30′ × 20′ × 20′) for 5 days *ad libitum* with free access to food and water. The oxygen concentration (85% oxygen) was maintained using Proox Oxygen Controller (BioSpherix, Lacona, NY). The oxygen mixture was humidified, and the concentration of CO_2 in the chamber was lower than 0.3%. Control mice were kept in room air.

Mouse Lung Experiments—Mice were anesthetized (pentobarbital, 90 mg/kg, intraperitoneal), and the trachea was intubated. The mice were then euthanized by using thoracotomy. The blood in pulmonary circulation was rinsed by infusing PBS through pulmonary artery. Then the lungs were removed and snap-frozen in liquid nitrogen for preparing homogenates. The assays of eNOS catalytic activity, protein tyrosine nitration, and co-immunoprecipitation of eNOS and β-actin were performed using the lung homogenates.

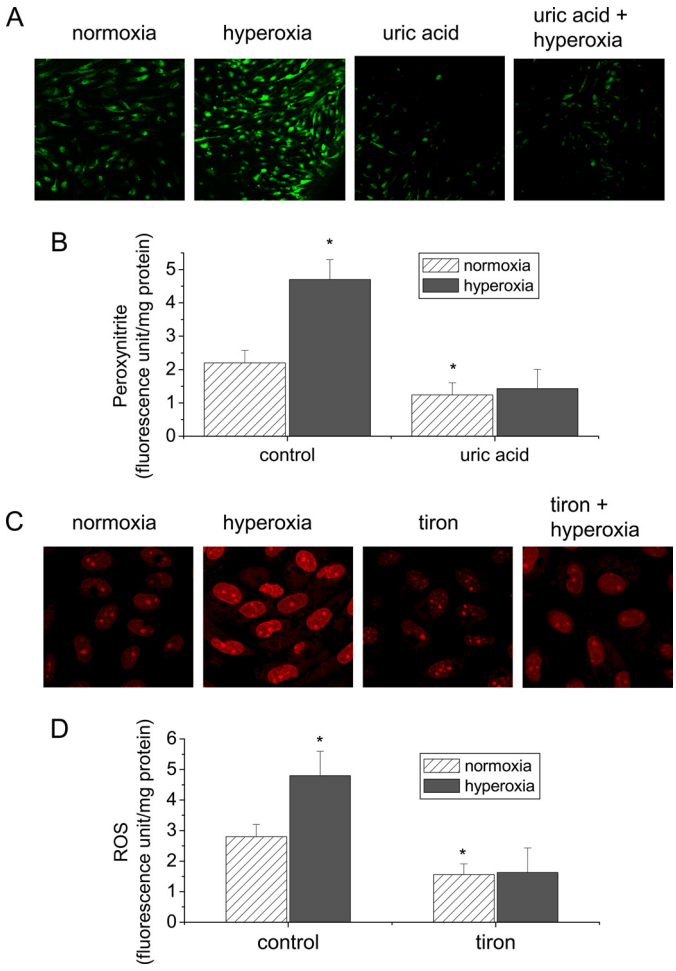

FIGURE 1. **Hyperoxia increases the formation of peroxynitrite and superoxide radicals in lung endothelial cells.** *A* and *B*, PAEC were exposed to 95% oxygen for 24 h in the presence or absence of uric acid (100 μM) and then loaded with APF (10 μM) for 30 min. The fluorescence images of cells were taken using a confocal laser scanning microscope LSM 510 (*A*). The fluorescence intensities were assayed by SpectraMax spectrophotometer using excitation 490 nm and emission 515 nm (*B*). *C* and *D*, PAEC were exposed to 95% oxygen for 24 h in the presence or absence of tiron (5 mM) and then loaded with DHE (10 μM) for 15 min. The fluorescence images of cells were taken using a confocal laser scanning microscope LSM 510 (*C*). The fluorescence intensities were assayed by SpectraMax spectrophotometer using excitation 510 nm and emission 590 nm (*D*). Results are expressed as mean ± S.D.; $n = 3$ experiments. *, $p < 0.05$ *versus* normoxia control.

Statistical Analysis—In each experiment, experimental and control cells were matched for cell line, age, seeding density, number of passages, and number of days postconfluence to avoid variation in tissue culture factors that can influence measurements of peroxynitrite, NO, and superoxide production. Results are shown as means ± S.D. for *n* experiments. One-way ANOVA and post *t* test analyses were used to determine the significance of differences between the means of different groups. $p < 0.05$ was considered statistically significant.

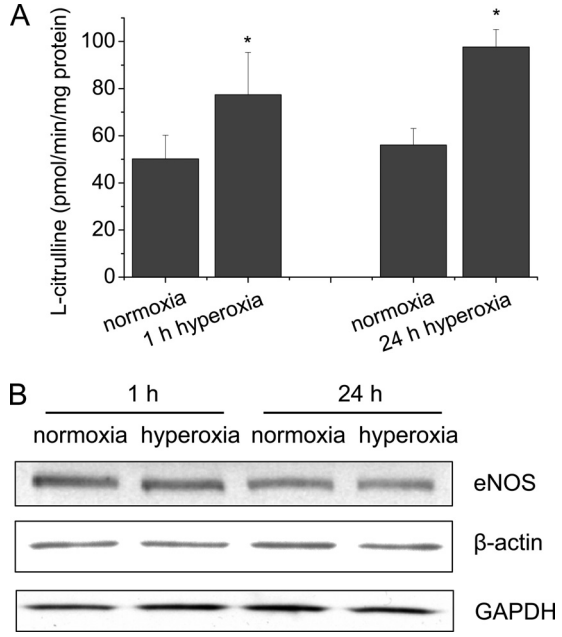

FIGURE 2. **The effects of hyperoxia on eNOS activity and protein contents of eNOS and β-actin in lung endothelial cells.** PAEC were exposed to 95% oxygen for 1–24 h. eNOS activities (*A*) and the protein contents (*B*) were measured as described under "Experimental Procedures." Results are expressed as mean ± S.D.; $n = 3$ experiments. *, $p < 0.05$ *versus* normoxia. Images are representative of three independent experiments.

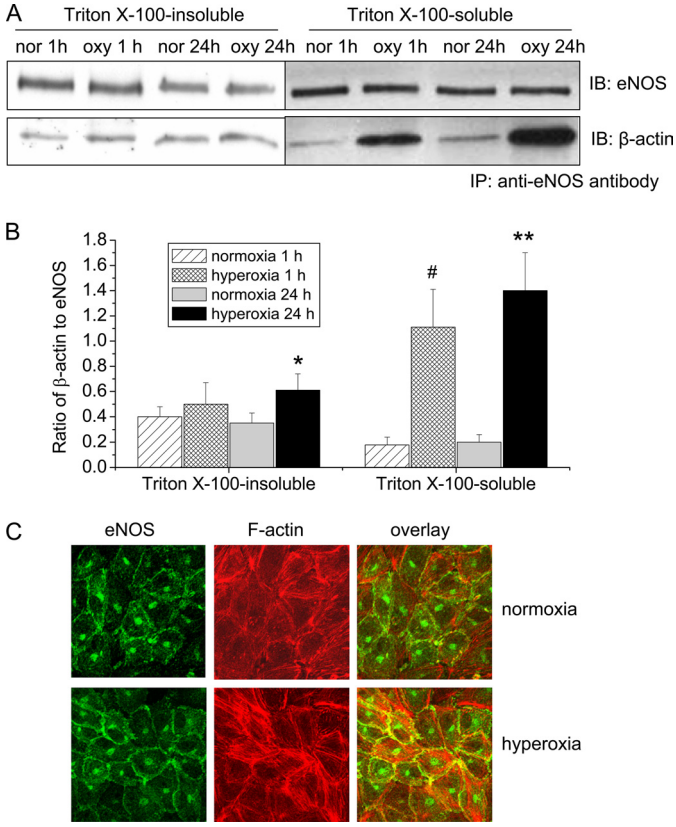

FIGURE 3. **The effects of hyperoxia on eNOS-actin association in PAEC.** *A* and *B*, PAEC were exposed to 95% oxygen for 1–24 h and then Triton X-100-insoluble and soluble fractions were separated and lysed in RIPA buffer. The cell lysates from the Triton X-100-insoluble and soluble fractions were subject to co-immunoprecipitation using anti-eNOS antibody as described under "Experimental Procedures." *A* is a representative blot from three separate experiments. *B* is a bar graph depicting the ratio of eNOS to β-actin protein in the immunoprecipitates. Results are expressed as mean ± S.D.; $n = 3$ experiments. *, $p < 0.05$ *versus* normoxia. *C*, PAEC were exposed to 95% oxygen for 24 h and then immuno-stained for eNOS (*green*) and F-actin (*red*). Images are representative of three independent experiments.

RESULTS

Hyperoxia Increases the Formation of Peroxynitrite and Superoxide in PAEC—To study the effect of hyperoxia on the formation of peroxynitrite, PAEC were exposed to 95% oxygen in the presence and absence of uric acid, a peroxynitrite scavenger, for 24 h. Peroxynitrite level in the cells was measured by using a peroxynitrite-specific fluorescence probe APF which does not react with NO, superoxide, and hydrogen peroxide (23). We found that the fluorescence level in cells exposed to hyperoxia was much higher than those exposed to normoxia (Fig. 1, *A* and *B*). The presence of uric acid prevented hyperoxia-induced increase in the fluorescence intensity (Fig. 1, *A* and *B*), suggesting that the fluorescence of APF is due to the increase in peroxynitrite formation. Thus, these results indicate that hyperoxia induces the formation of peroxynitrite in lung endothelial cells.

To investigate whether hyperoxia increases ROS formation, the level of $O_2^{\cdot-}$ was determined by using the fluorescent dye dihydroethidium (DHE) as previously reported (25). In the presence of $O_2^{\cdot-}$, DHE is converted to the fluorescent molecule hydroethidium and ethidium. Both products intercalate with DNA that can be detected by fluorescence confocal microscopy and fluorescence spectroscopy. As shown in Fig. 1, *C* and *D*, exposure of PAEC to hyperoxia for 24 h led to an increase in the fluorescence intensity. Superoxide radical scavenger tiron prevented the increase in the fluorescence intensity in hyperoxic PAEC (Fig. 1, *C* and *D*). These data suggest that exposure to hyperoxia increases superoxide radical level in lung endothelial cells.

Exposure of PAEC to Hyperoxia Increases eNOS Activity—To study the role of eNOS in the hyperoxia-induced increase in peroxynitrite formation in lung endothelial cells, eNOS activity were measured in normoxic and hyperoxic PAEC. As shown in Fig. 2*A*, exposure of PAEC to 95% of oxygen for 1 to 24 h caused an increase in eNOS activity. However, the eNOS protein contents in hyperoxic PAEC remained unchanged (Fig. 2*B*), suggesting that hyperoxia increases eNOS activity through a post-translational mechanism.

Effect of Hyperoxia on eNOS-β-Actin Association in PAEC—We have reported that eNOS is associated with β-actin in endothelial cells and that association of eNOS with β-actin increases eNOS activity and NO production (18–20). To study the role of eNOS-β-actin interaction in hyperoxia-induced increase in the formation of peroxynitrite, eNOS-β-actin association was evaluated in hyperoxic and normoxic PAEC using co-immunoprecipitation and confocal microscopy. As shown in Fig. 3, *A* and *B*, exposure of PAEC with hyperoxia for 1 h significantly increased the amount of β-actin co-immunoprecipitated with eNOS in the Triton X-100 soluble fraction which contains mainly G-actin. The increased association of eNOS and G-actin lasted for 24 h. Meanwhile, hyperoxia for 24 h increased the amount of β-actin co-immunoprecipitated with eNOS in the Triton X-100 insoluble fraction which contains mainly F-actin (Fig. 3, *A* and *B*). Consistent with this result, confocal microscopy

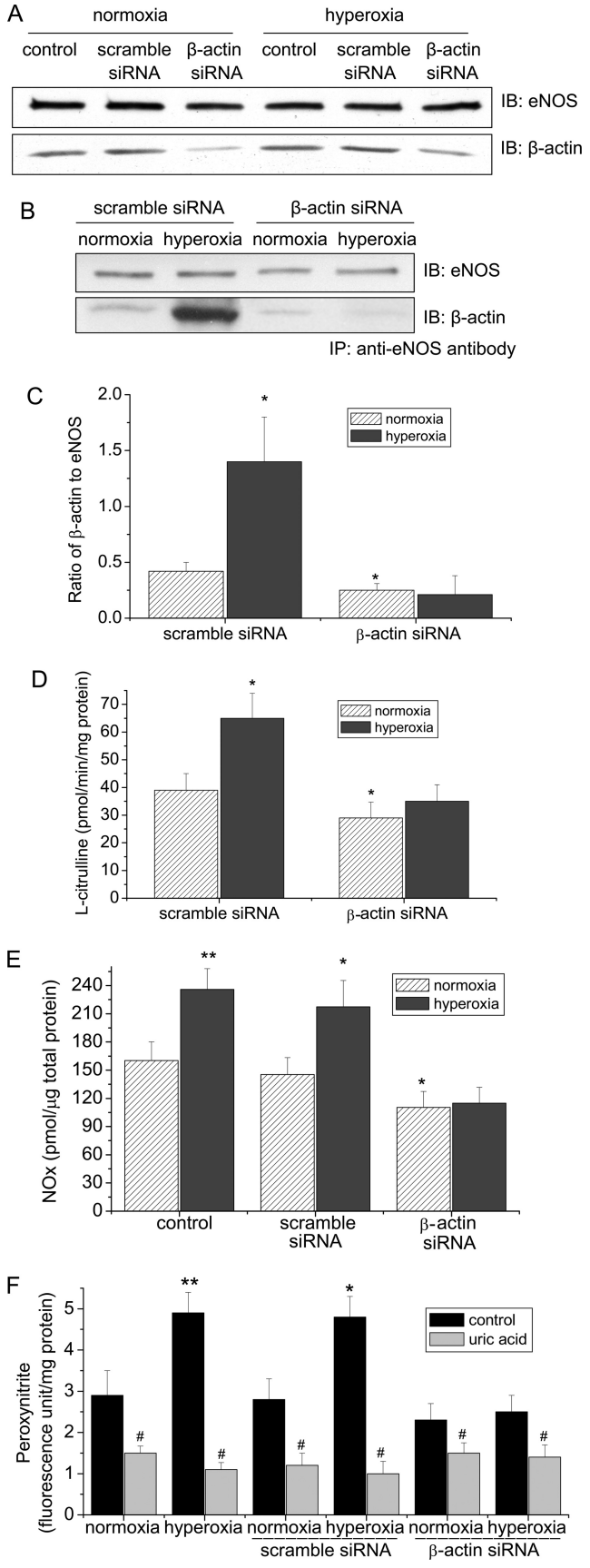

FIGURE 4. **Reducing β-actin availability prevents hyperoxia-induced increases in eNOS-β-actin association, eNOS activity, and formation of NO and peroxynitrite.** PAEC were transfected with a scramble siRNA or a siRNA against β-actin. After 48 h, the cells were exposed to normoxia or hyperoxia (95% oxygen) for 24 h. Then, the protein contents of eNOS and β-actin (*A*) and eNOS-β-actin association (*B* and *C*), eNOS activity (*D*), NO (*E*), and peroxynitrite (*F*) were determined as described under "Experimental Procedures." *A* and *B* are representative immunoblots from three experiments. *C* is a bar graph showing the changes in the ratio of eNOS to β-actin in the immunoprecipitates. Results are expressed as mean ± S.D.; n = three experiments. *, $p < 0.05$ *versus* normoxia in scramble siRNA group. **, $p < 0.05$ *versus* normoxia group; #, $p < 0.05$ *versus* control (without uric acid).

revealed that there was an increased co-localization of eNOS and cortical F-actin at plasma membrane in hyperoxic PAEC (Fig. 3*C*). These data indicate that hyperoxia increases eNOS association with both G-actin and F-actin in lung endothelial cells.

Reducing β-Actin Availability Prevents Hyperoxia-induced Increases in eNOS-β-Actin Association, eNOS Activity, and the Formation of NO and Peroxynitrite—To further analyze the role of eNOS-β-actin interaction in hyperoxia-induced increase in the formation of NO and peroxynitrite, eNOS-β-actin association was disrupted by reducing β-actin availability in PAEC using siRNA technology as previously reported by us (18). As shown in Fig. 4*A*, transfection of PAEC with β-actin siRNA resulted in a decrease in β-actin protein level by nearly 70% at both normoxic and hypoxic conditions. Silencing β-actin did not cause cellular injury to PAEC (18). Interestingly, hyperoxia failed to induce an increase in the amount of β-actin co-immunoprecipitated with eNOS in PAEC transfected with β-actin siRNA (Fig. 4, *B* and *C*). In addition, reducing β-actin availability prevented hyperoxia-induced increase in eNOS activity (Fig. 4*D*). These data indicate that inhibition of eNOS-β-actin association prevents hyperoxia-induced increase in eNOS activity. We then measured NO and peroxynitrite production in endothelial cells in which eNOS-β-actin association was disrupted by β-actin siRNA. In the presence of scramble siRNA, exposure of PAEC to hyperoxia induced a remarkable increase in NO and peroxynitrite formation (Fig. 4, *E* and *F*). Transfection of endothelial cells with β-actin siRNA significantly inhibited hyperoxia-induced increases in the formation of NO and peroxynitrite (Fig. 4, *E* and *F*).

Synthetic Peptide P326TAT Prevents eNOS-β-Actin Association, Peroxynitrite Formation, and Protein Tyrosine Nitration in Hyperoxia-exposed PAEC—We have shown that peptide P326TAT specifically binds to β-actin and competitively inhibits eNOS-β-actin association *in vitro* and in intact endothelial cells (21). To study whether peptide P326TAT prevents hyperoxia-induced increase in eNOS-β-actin association, endothelial cells were transfected with peptide 326 linked to an 11-amino acid transduction domain of HIV TAT (P326TAT) as described by Gustafsson *et al.* (25). This TAT tag is a novel method used to facilitate delivery of biologically active proteins or peptides into cells and tissues through the fusion of a protein transduction domain to the protein or peptide of interest (26). We have shown that P326TAT and control peptide PlwTAT can enter endothelial cells efficiently (21). As shown in Fig. 5, *A* and *B*, incubation of endothelial cells with peptide P326TAT significantly decreased the amount of β-actin co-immunoprecipitated with eNOS and prevented hyperoxia-induced increase in eNOS-β-actin co-immunoprecipitation. We then

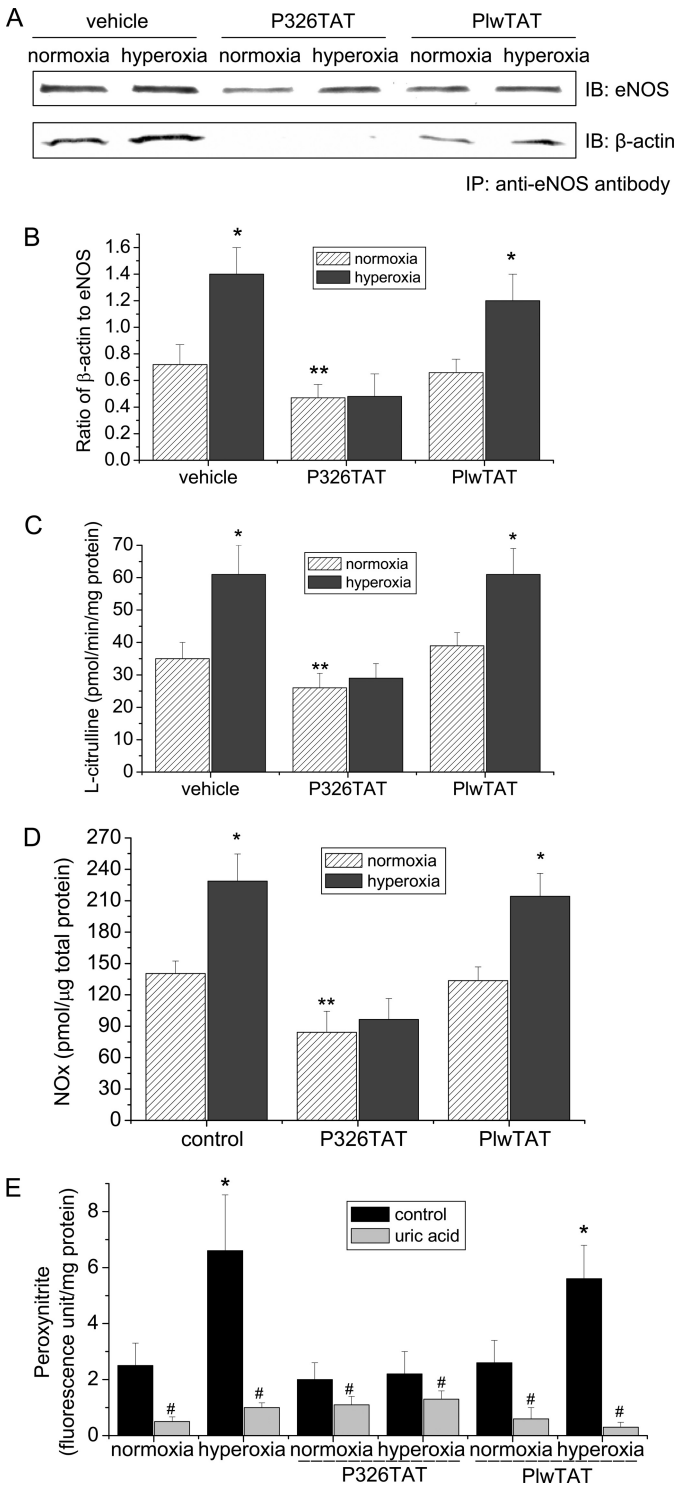

FIGURE 5. **Synthetic peptide P326TAT blocks eNOS-β-actin interaction and hyperoxia-induced increase in eNOS activity.** PAEC were incubated with or without P326TAT and PlwTAT at final concentration 20 μM and then exposed to normoxia or hyperoxia (95% oxygen) for 24 h. eNOS-β-actin association (*A* and *B*), eNOS activity (*C*), NO (*D*), and peroxynitrite (*E*) were determined as described under "Experimental Procedures." *A* is a representative immunoblot from three experiments. *B* is a bar graph showing the changes in the ratio of eNOS to β-actin in the immunoprecipitates. Results are expressed as mean ± S.D.; $n = 3$ experiments. *, $p < 0.05$ *versus* normoxia; **, $p < 0.05$ *versus* normoxia in PlwTAT group; #, $p < 0.05$ *versus* control (without uric acid).

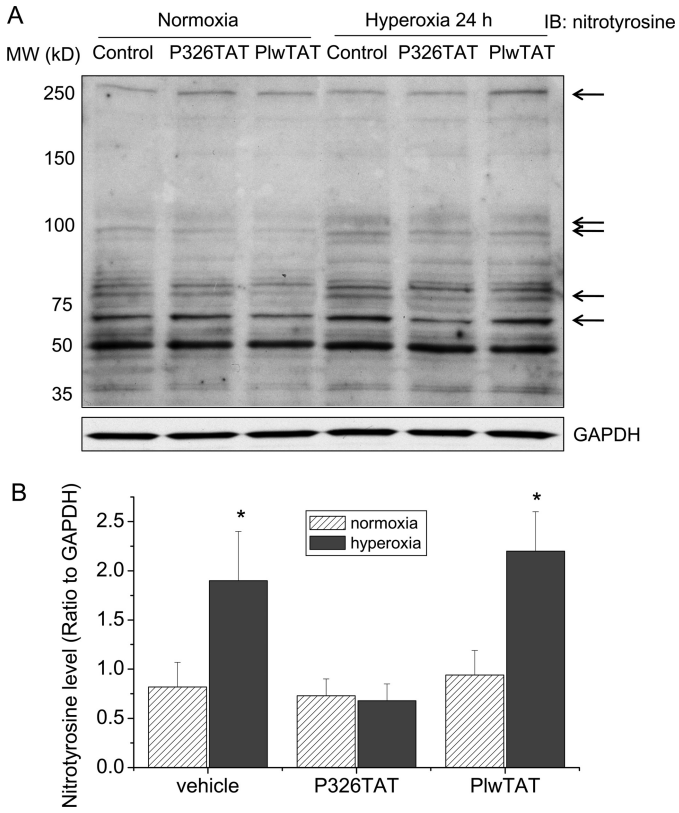

FIGURE 6. **Synthetic peptide P326TAT blocks hyperoxia-induced increase in protein tyrosine nitration.** PAEC were exposed to normoxia or hyperoxia (95% oxygen) in the presence and absence of P326TAT and PlwTAT at final concentration 20 μM for 24 h. Then, protein tyrosine nitration was assayed as described under "Experimental Procedures." *A* is a representative immunoblot from three experiments. *B* is a bar graph showing the changes in tyrosine nitration of proteins at 250, 100, 75, and 60 kDa. Results are expressed as mean ± S.D.; $n = 3$ experiments. *, $p < 0.05$ *versus* normoxia group.

measured eNOS activity, NO and peroxynitrite production in P326TAT-transfected endothelial cells exposed to normoxic and hyperoxic conditions. As shown in Fig. 5*C*, hyperoxic exposure did not induce an increase in eNOS activity in P326TAT-transfected cells, comparing to cells transfected with control peptide PlwTAT. Moreover, P326TAT prevented hyperoxia-induced increases in NO and peroxynitrite formation (Fig. 5, *D* and *E*). Furthermore, to study whether alterations in peroxynitrite formation lead to changes in protein tyrosine nitration, protein nitrotyrosine in PAEC treated with or without PlwTAT and P326TAT under normoxic and hyperoxic conditions was assayed. As shown in Fig. 6, hyperoxia induced the increases in tyrosine nitration of proteins at 250, 100, 75, and 60 kDa in PAEC treated with or without control peptide PlwTAT. The levels of tyrosine nitration proteins at 250, 100, 75, and 60 kDa in PAEC treated with P326TAT were comparable between normoxia and hyperoxia (Fig. 6). These results show that peptide P326TAT prevents hyperoxia-induced increases in eNOS-β-actin association, eNOS activity, the formation of NO and peroxynitrite, and protein tyrosine nitration in PAEC.

Mutation of β-Actin Binding Domain in eNOS Protein Prevents Hyperoxia-induced eNOS-β-Actin Association and Peroxynitrite Formation—The hydrophobic amino acids residues leucine 326, leucine 328, tryptophan 330, and leucine 333 within β-actin binding domain of eNOS are critical for eNOS-

β-actin interaction (21). To further study the role of eNOS-β-actin interaction in hyperoxia-induced increase in peroxynitrite formation, residues leucine 326, leucine 328, tryptophan 330, and leucine 333 in the β-actin binding domain of eNOS were replaced for alanine by site-directed mutagenesis. The plasmids containing wild type and mutant eNOS genes were transfected into COS-7 cells. As shown in Fig. 7, *A* and *B*, hyperoxia increased the amount of β-actin co-precipitated with eNOS in COS-7 cells transfected with the plasmids containing wild-type eNOS gene but failed to increase the amount of β-actin co-precipitated with eNOS mutant in COS-7 cells transfected with the plasmids containing eNOS mutant gene. More importantly, the increases in eNOS activity and the formation of NO and peroxynitrite induced by hyperoxia were prevented in COS-7 cells containing eNOS mutant gene (Fig. 7, *C–E*). The inhibition of hyperoxia-induced increase in NO and peroxynitrite generation in COS-7 cells containing eNOS mutant gene are not due to the direct effect of the mutation on eNOS activity, because the catalytic activity from purified wild type and mutated eNOS were comparable (21). Taken together, these results indicate that disruption of eNOS-β-actin association prevents hyperoxia-induced increases in eNOS activity and the formation of NO and peroxynitrite.

Hyperoxia Induces Increases in eNOS-β-Actin Association, eNOS Activity, and Protein Tyrosine Nitration in Mouse Lungs—To study whether hyperoxia causes alterations in eNOS-β-actin association, eNOS activity, and protein tyrosine nitration in mouse lungs, male C57BL/6 mice were exposed to 85% oxygen for 5 days, then eNOS-β-actin association, eNOS activity, and protein nitrotyrosine were assayed in the lung homogenates. As shown in Fig. 8, *A* and *B*, the eNOS protein contents were comparable between normoxic and hyperoxic lungs. However, the amount of β-actin co-immunoprecipitated with eNOS was much larger in the homogenates from hyperoxic lungs than those from normoxic lungs, suggesting that hyperoxia induces an increase in eNOS-β-actin association in mouse lungs. Correspondingly, eNOS activities were much higher in hyperoxic lungs than in normoxic lungs (Fig. 8*C*). Furthermore, nitrotyrosine protein contents were much higher in hyperoxic lungs than those in normoxic lungs (Fig. 8, *D* and *E*). These data indicate that hyperoxia induces increases in eNOS-β-actin association, eNOS activity, and protein tyrosine nitration in mouse lungs.

DISCUSSION

The major finding in this study is that hyperoxia increases eNOS-β-actin association, eNOS activity, NO production, peroxynitrite formation, and protein tyrosine nitration in lung endothelial cells and in mouse lungs. We also showed that disruption of eNOS-β-actin interaction inhibited hyperoxia-induced increase in eNOS activity and NO and peroxynitrite production in lung endothelial cells. This novel discovery indicates that eNOS-β-actin association contributes to hyperoxia-induced increases in peroxynitrite formation and protein tyrosine nitration in lung endothelial cells.

Exposure of lung endothelial cells to high concentration of oxygen leads to accumulation of large amount of ROS. The source of hyperoxia-induced ROS production might be the

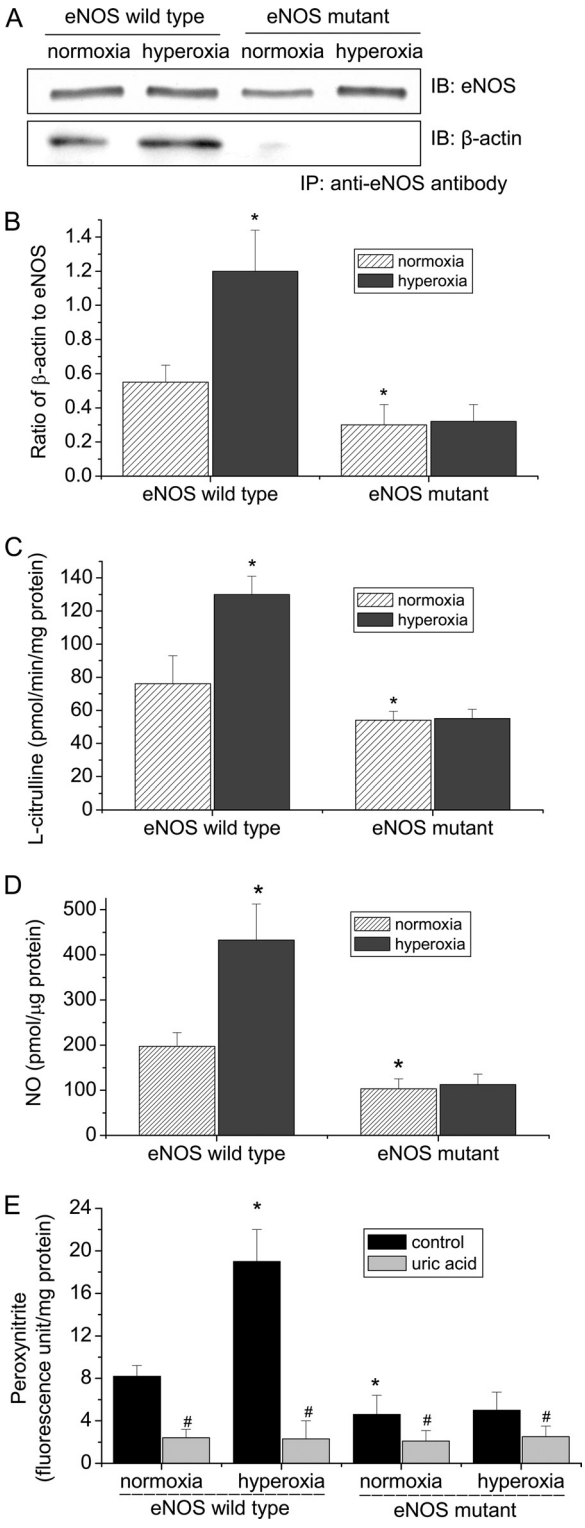

FIGURE 7. **Mutation of the β-actin binding domain in eNOS protein prevents eNOS-β-actin association and hyperoxia-induced increase in eNOS activity in COS-7 cells.** COS-7 cells transfected with wild type and mutant eNOS plasmids were exposed to normoxia or hyperoxia (95% oxygen) for 24 h. Then, eNOS-β-actin association (*A* and *B*), eNOS activity (*C*), NO (*D*), and peroxynitrite (*E*) were determined as described under "Experimental Procedures." *A* is a representative immunoblot from three experiments. *B* is a bar graph showing the changes in the ratio of eNOS to β-actin in the immunoprecipitates. Results are expressed as mean ± S.D.; $n = 3$ experiments. *, $p < 0.05$ *versus* normoxia in wild-type group; #, $p < 0.05$ *versus* control (without uric acid).

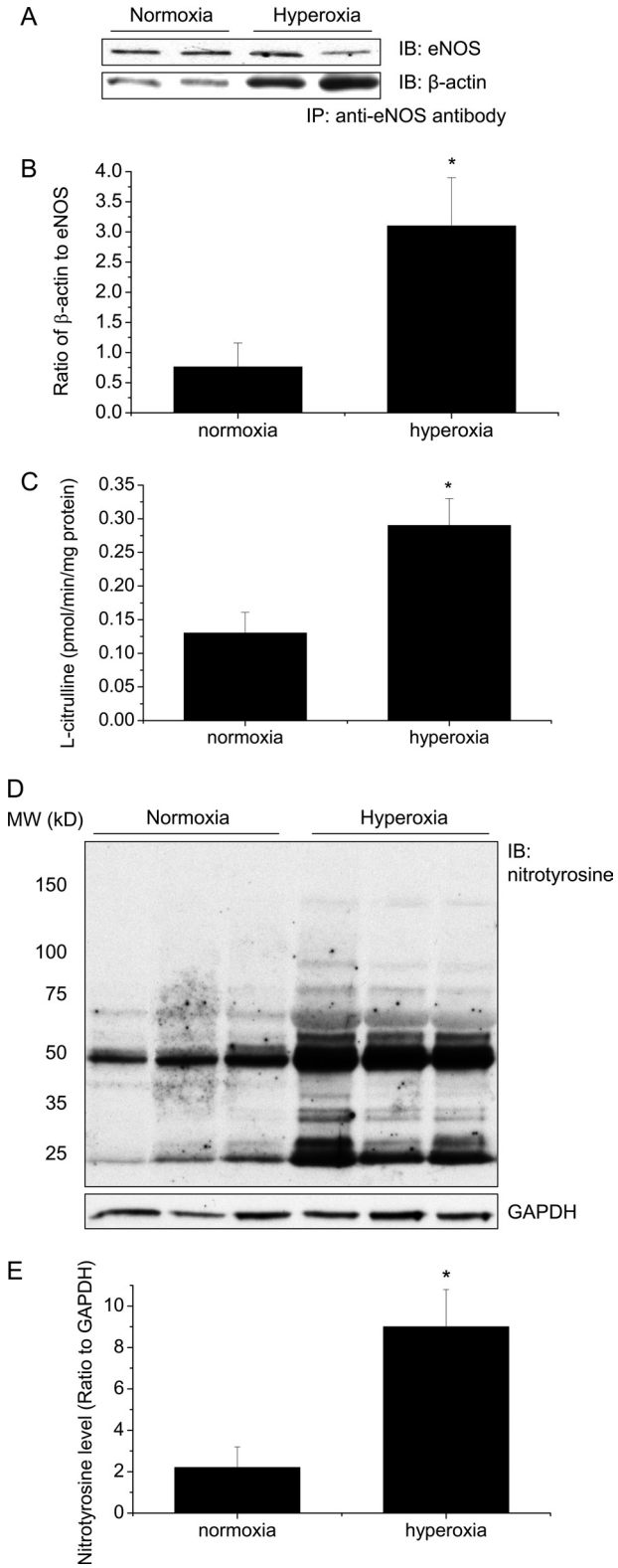

FIGURE 8. **Hyperoxia increases eNOS-β-actin association, eNOS activity, and protein tyrosine nitration in mouse lungs.** Male C57BL/6 mice were exposed to 85% oxygen for 5 days, then eNOS-β-actin association (*A* and *B*), eNOS activity (*C*), and protein nitrotyrosine (*D* and *E*) were assayed in the lung homogenates as described under "Experimental Procedures." *A* and *D* are representative immunoblots from 10 experiments. *B* is a bar graph showing the changes in the ratio of eNOS to β-actin in the immunoprecipitates. *E* is a bar graph showing the changes in protein tyrosine nitration. Results are expressed as mean ± S.D.; $n = 10$ experiments. *, $p < 0.05$ *versus* normoxia control.

mitochondrial electron transport (26) or NADPH oxidase-catalyzed reaction (27, 28). The superoxide radicals react rapidly with NO generated by eNOS and form more potent oxidizing reactive nitrogen species such as peroxynitrite. eNOS plays an important role in the formation of peroxynitrite in endothelial cells during hyperoxia (9, 10). Inhibition of eNOS using L-NAME or knock-out of eNOS reduces peroxynitrite-mediated cytotoxicity in hyperoxic retinal damage (9, 11). However, the mechanism for hyperoxia-induced alterations in eNOS activity and NO release has not been clarified. We found that exposure of PAEC to 95% oxygen caused increases in eNOS activity and in the formation of peroxynitrite and NO without changes in eNOS protein contents, suggesting that hyperoxia modulates eNOS activity via a posttranslational mechanism. Protein-protein interaction and phosphorylation represent the most important post-translational mechanism for eNOS regulation. Our data demonstrate that the amount of Hsp90 co-precipitated with eNOS was comparable between normoxic and hyperoxic cells (supplemental Fig. S1). Moreover, phosphorylation of eNOS on Thr-495 and Ser-1177 did not change significantly during hyperoxia (supplemental Fig. S1). Therefore, eNOS interaction with Hsp90 and phosphorylations of eNOS are unlikely to be involved in hyperoxia-induced increase in peroxynitrite generation. Interestingly, we have recently reported that β-actin interacts with eNOS and this interaction increases eNOS activity and NO release (18–20). In the present study, we found that hyperoxia enhanced the co-localization of eNOS with cortical F-actin in PAEC as evidenced by immunofluorescence confocal microscopy. Exposure of PAEC to hyperoxia also significantly increased the amount of β-actin co-immunoprecipitated with eNOS in the Triton X-100 soluble and insoluble fractions. Reduction of β-actin availability by β-actin siRNA decreased hyperoxia-induced association of eNOS with β-actin as well as NO and peroxynitrite formation, indicating a critical role of eNOS-β-actin association in hyperoxia-induced peroxynitrite generation.

Hyperoxia-induced increase in eNOS-β-actin association in PAEC could be caused by alterations in the affinity between eNOS and β-actin. Notably, the actin binding site on eNOS protein has been identified as being at amino acid residues 326–333 and hydrophobic residues leucine 326, leucine 328, tryptophan 330, and leucine 333 in the actin binding site are essential for actin binding (21). Our data indicate that a synthetic peptide P326TAT which contains a sequence of actin binding site on eNOS inhibits eNOS-β-actin association and prevents hyperoxia-induced increase in NO and peroxynitrite generation. But the control peptide PlwTAT, in which residues leucine 326, leucine 328, tryptophan 330, and leucine 333 are replaced by alanine, in the same concentrations does not affect hyperoxia-induced increase in eNOS-β-actin association and in the generation of NO and peroxynitrite. Furthermore, mutation of residues leucine 326, leucine 328, tryptophan 330, and leucine 333 for neutral alanine results in inhibitions of hyperoxia-dependent eNOS-β-actin association and NO and peroxynitrite generation. These results indicate that hyperoxia may increase the affinity between eNOS and β-actin, leading to the increased formation of NO and peroxynitrite in lung endothelial cells.

The mechanisms for hyperoxia-induced alterations in the affinity of β-actin to eNOS are not clear. Hyperoxia causes actin cytoskeletal rearrangement and tyrosine phosphorylation of cortactin (28). Hyperoxia may induce modifications such as oxidation/peroxidation and/or phosphorylation of residues in the actin-binding site on eNOS or the eNOS binding site on β-actin, which may affect eNOS-β-actin association (29, 30). Further studies are necessary to clarify these possibilities.

Lung vascular endothelial alterations represent the most striking pathophysiological changes in hyperoxia-induced lung injuries. Our observations show that mouse lungs exposed to hyperoxia exhibit increases in eNOS-β-actin association and eNOS activity. Protein tyrosine nitration is also increased in hyperoxic mouse lungs. These data suggest that peroxynitrite formation caused by increased eNOS activity because of eNOS-β-actin association may play important role in lung vascular endothelial damage in hyperoxic lung injuries.

The increase in NO and peroxynitrite production in PAEC and mouse lungs exposed to hyperoxia could be contributed by changes in other NOS isoforms besides eNOS. Nevertheless, others have reported that lung endothelium does not express neuronal NOS (nNOS) (31). Similarly, inducible NOS (iNOS) expression is not detectable in PAEC (32). We did not observe alterations of nNOS and iNOS in the normoxic and hyperoxic lungs (supplemental Fig. S2). In line with this finding, Kobayashi reported that knock-out of iNOS does not affect protein tyrosine nitration in hyperoxic mouse lung and that peroxynitrite generation during hyperoxia is independent of iNOS (33). Therefore, nNOS and iNOS may not contribute to hyperoxia-induced increases in NO and peroxynitrite production in PAEC and mouse lungs.

In summary, this study has provided novel evidence showing that eNOS-β-actin association contributes to increased peroxynitrite formation in lung endothelial cells during hyperoxia. Manipulation of eNOS-β-actin association may render novel therapeutic method to treat diseases associated to hyperoxic injuries.

REFERENCES

1. Berkowitz, D. S., and Coyne, N. G. (2003) *Crit. Care Nurs. Q.* **26,** 28–34
2. Siflinger-Birnboim, A., and Johnson, A. (2003) *Am. J. Physiol. Lung Cell Mol. Physiol.* **284,** L435–L451
3. De Backer, T. L., Smedema, J. P., and Carlier, S. G. (2001) *BioDrugs.* **15,** 801–817
4. Palevsky, H. I., and Fishman, A. P. (1991) *JAMA* **265,** 1014–1020
5. Imperatore, F., Cuzzocrea, S., Luongo, C., Liguori, G., Scafuro, A., De Angelis, A., Rossi, F., Caputi, A. P., and Filippelli, A. (2004) *Intensive Care Med.* **30,** 1175–1181
6. MacFarlane, C., Cronje, F. J., and Benn, C. A. (2000) *J. R. Army Med. Corps.* **146,** 185–190
7. Brueckl, C., Kaestle, S., Kerem, A., Habazettl, H., Krombach, F., Kuppe, H., and Kuebler, W. M. (2006) *Am. J. Respir. Cell Mol. Biol.* **34,** 453–463
8. Radomski, A., Sawicki, G., Olson, D. M., and Radomski, M. W. (1998) *Br. J. Pharmacol.* **125,** 1455–1462
9. Gu, X., El-Remessy, A. B., Brooks, S. E., Al Shabrawey, M., Tsai, N. T., and Caldwell, R. B. (2003) *Am. J. Physiol. Cell Physiol.* **285,** C546–C554
10. Li, L. F., Liao, S. K., Lee, C. H., Huang, C. C., and Quinn, D. A. (2007) *Crit. Care* **11,** R89
11. Brooks, S. E., Gu, X., Samuel, S., Marcus, D. M., Bartoli, M., Huang, P. L., and Caldwell, R. B. (2001) *Invest. Ophthalmol. Vis. Sci.* **42,** 222–228
12. Su, Y., Kondrikov, D., and Block, E. R. (2005) *Cell Biochem. Biophys.* **43,** 439–449
13. Michel, T., and Feron, O. (1997) *J. Clin. Invest.* **100,** 2146–2152
14. Ju, H., Venema, V. J., Marrero, M. B., and Venema, R. C. (1998) *J. Biol. Chem.* **273,** 24025–24029
15. García-Cardeña, G., Fan, R., Shah, V., Sorrentino, R., Cirino, G., Papapetropoulos, A., and Sessa, W. C. (1998) *Nature* **392,** 821–824
16. Su, Y., and Block, E. R. (2000) *Am. J. Physiol. Lung Cell Mol. Physiol.* **278,** L1204–L1212
17. Cao, S., Yao, J., and Shah, V. (2003) *J. Biol. Chem.* **278,** 5894–5901
18. Kondrikov, D., Han, H. R., Block, E. R., and Su, Y. (2006) *Am. J. Physiol. Lung Cell Mol. Physiol.* **290,** L41–L50
19. Su, Y., Edwards-Bennett, S., Bubb, M. R., and Block, E. R. (2003) *Am. J. Physiol. Cell Physiol.* **284,** C1542–C1549
20. Su, Y., Kondrikov, D., and Block, E. R. (2007) *Sci. STKE.*, e52–1–e52–3
21. Kondrikov, D., Fonseca, F. V., Elms, S., Fulton, D., Black, S. M., Block, E. R., and Su, Y. (2010) *J. Biol. Chem.* **285,** 4319–4327
22. Su, Y., Han, W., Giraldo, C., De Li, Y., and Block, E. R. (1998) *Am. J. Respir. Cell Mol. Biol.* **19,** 819–825
23. Saito, S., Yamamoto-Katou, A., Yoshioka, H., Doke, N., and Kawakita, K. (2006) *Plant Cell Physiol.* **47,** 689–697
24. Church, J. E., and Fulton, D. (2006) *J. Biol. Chem.* **281,** 1477–1488
25. Carter, W. O., Narayanan, P. K., and Robinson, J. P. (1994) *J. Leukoc. Biol.* **55,** 253–258
26. Li, J., Gao, X., Qian, M., and Eaton, J. W. (2004) *Free Radic. Biol. Med.* **36,** 1460–1470
27. Parinandi, N. L., Kleinberg, M. A., Usatyuk, P. V., Cummings, R. J., Pennathur, A., Cardounel, A. J., Zweier, J. L., Garcia, J. G., and Natarajan, V. (2003) *Am. J. Physiol. Lung Cell Mol. Physiol.* **284,** L26-L38
28. Usatyuk, P. V., Romer, L. H., He, D., Parinandi, N. L., Kleinberg, M. E., Zhan, S., Jacobson, J. R., Dudek, S. M., Pendyala, S., Garcia, J. G., and Natarajan, V. (2007) *J. Biol. Chem.* **282,** 23284–23295
29. Dalle-Donne, I., Rossi, R., Giustarini, D., Gagliano, N., Lusini, L., Milzani, A., Di, Simplicio, P., and Colombo, R. (2001) *Free Radic. Biol. Med.* **31,** 1075–1083
30. Dalle-Donne, I., Rossi, R., Milzani, A., Di, Simplicio, P., and Colombo, R. (2001) *Free Radic. Biol. Med.* **31,** 1624–1632
31. Fagan, K. A., Tyler, R. C., Sato, K., Fouty, B. W., Morris, K. G., Jr., Huang, P. L., McMurtry, I. F., and Rodman, D. M. (1999) *Am. J. Physiol.* **277,** L472–L478
32. Zhang, J., Patel, J. M., Li, Y. D., and Block, E. R. (1997) *Res. Commun. Mol. Pathol. Pharmacol.* **96,** 71–87
33. Kobayashi, H., Hataishi, R., Mitsufuji, H., Tanaka, M., Jacobson, M., Tomita, T., Zapol, W. M., and Jones, R. C. (2001) *Am. J. Respir. Cell Mol. Biol.* **24,** 390–397